Journal of Applied Fluid Mechanics, Vol. 17, No. 1, pp. 261-272, 2024.
Available online at www.jafmonline.net, ISSN 1735-3572, EISSN 1735-3645.
https://doi.org/10.47176/jafm.17.1.1922

On an Efficient Solution of the Boltzmann Equation Using the Modified Time Relaxed Monte Carlo (MTRMC) Scheme

M. Eskandari and S. S. Nourazar†

Department of Mechanical Engineering, Amirkabir University of Technology, Tehran, Iran

†*Corresponding Author Email: icp@aut.ac.ir*

ABSTRACT

The study proposes a new method called MTRMC to simulate flow in rarefied regimes, which are important in various industrial and engineering applications. This new method utilizes a modified collision function with smaller number of inter-molecular collisions, making it more computationally efficient than the widely used direct simulation Monte Carlo (DSMC) method. The MTRMC method is used to analyze the flow over a flat nano-plate at various free stream velocities, ranging from low to supersonic speeds. The results are compared with those from DSMC and time relaxed Monte Carlo (TRMC) schemes, and the findings show that the MTRMC method is in good agreement with the standard schemes, with a significant reduction in computational expense, up to 51% in some cases.

Article History

Received April 6, 2023
Revised August 5, 2023
Accepted September 12, 2023
Available online November 1, 2023

Keywords:

Boltzmann equation,
DSMC method,
TRMC method,
MTRMC method,
Taylor series expansion,
Nano-plate

1. INTRODUCTION

Studies show that in rarefied flows or micro- and nano-scale geometries, in which the characteristic length of a flow is similar in size to the mean free path, the Navier-Stokes equations cannot be applied for accurately simulating the flow. In these cases, the NS equations lose their validity and the Boltzmann equation should be solved as the governing equation (Cercignani & Cercignani, 1988; Bird, 1994). Since the development of the direct simulation Monte Carlo (DSMC) method, this method has been widely employed for numerically solving the Boltzmann equation in a wide variety of problems and geometries (Cercignani & Cercignani, 1988; Bird, 1994; Pareschi & Trazzi, 2005). Although the DSMC scheme is relatively straightforward and accurate, its significant computational cost is not justifiable. This issue is especially more pronounced in low-Knudsen flows. Therefore, it is of significant importance to develop modified approach to alleviate the CPU time of solving the governing equations (Gabetta et al., 1997; Oran et al., 1998; Pan et al., 2000; Filbet & Russo, 2003; Pareschi & Trazzi, 2005).

Aiming at resolving this shortcoming, a new and efficient numerical method called the time-relaxed Monte Carlo (TRMC) method was developed, which can be used for a wide range of Knudsen numbers. In this method, the Wild sum expansion (Wild, 1951) is used to incorporate time discretization, and a local Maxwellian distribution is applied to particles rather than performing complex calculations to simulate high-order collisions (Pareschi & Caflisch, 1999). Consequently, this method has a simple and effective algorithm. Pareschi & Russo (2000) analyzed the stability of the TRMC approach and demonstrated its A-stability and L-stability in numerous case studies. They also applied the TRMC scheme to perform numerical simulations and obtain a reasonable solution for the Kac equation, and achieved promising results when compared with the DSMC method. The TRMC scheme has been subject to stability analysis by Pareschi and Russo, and their findings in numerous case studies demonstrated that the scheme is both A-stable and L-stable. Additionally, Pareschi & Russo (2001a, 2001b) and; Pareschi and Wennberg 2001) modified the TRMC algorithm for variable hard sphere (VHS) particles, investigated the 1D shock wave problem, and achieved promising data. Pareschi and Trazzi (2005) developed higher orders of the TRMC approach to simulate gas flow around an obstacle and demonstrated significantly lower computational expenses when compared to the DSMC method. Aiming at improving the simulation accuracy, Russo et al. (2005) performed similar modifications and developed the TRMC3 scheme, where 3 implies third-

order collisions. In this regard, they studied Couette flow at various rarefaction degrees and wall velocities as the benchmark case study. The comparison of hydrodynamic parameters obtained from the different schemes demonstrated that the results from the TRMC method conform to those from the DSMC approach. Ganjaei and Nourazar (2009) conducted a study on the flow of a binary mixture of Argon and Helium in a rotating cylinder. Since the operating gas was a mixture of two gases, Dalton's law was applied to determine the partial pressures of species. It was found that the predictions using the TRMC method conform to the analytical solution. It was revealed that the TRMC scheme can be used to perform accurate simulations in complex geometries. Trazzi et al. (2009) proposed a recursive TRMC algorithm to achieve uniform time accuracy, which is not affected by the time step. Through the proposed algorithm, CPU time of simulating both homogeneous and non-homogeneous problems were reduced remarkably when compared to that of the DSMC scheme. Dimarco and Pareschi (2011) proposed a class of exponential Runge-Kutta integration methods for kinetic equations, specifically addressing the challenges associated with solving nonlinear equations in stiff regimes. These methods offer exact treatment of relaxation operators, avoidance of nonlinear systems, stability, negativity, and entropy inequality. In addition to being suitable for deterministic techniques, the developed methods are also applicable to probabilistic numerical approaches. They also examined the applicability, advantages, and limitations of the developed methods. Eskandari and Nourazar (2017; 2018a) utilized various orders of the TRMC approach to investigate the behavior of microcavity flow under different conditions such as varying lid velocities and rarefaction degrees. Meanwhile, they also applied the TRMC scheme to analyze a nano-plate subjected to various free stream velocities and rarefaction degrees. Based on the performed simulations, it was demonstrated that the TRMC scheme can accurately predict the behavior of rarefied gas flows for a wide range of Knudsen numbers and geometries, with reduced computational cost compared to the DSMC method. To decrease computational costs, a modified version of the TRMC scheme (MTRMC) was suggested by Eskandari and Nourazar (2018 a, b). The MTRMC was then utilized to study the flow within a lid-driven micro-cavity, and a reduction in computational time of up to 51% was achieved. Baliti et al. (2019) investigated the heat transfer of rarefied gas confined within a square cavity using DSMC and Navier-Stokes-Fourier (NSF) methods. Plimpton et al. (2019) developed the open-source SPARTA DSMC code and simulated numerous benchmark problems. Mukherjee et al. (2019) studied the influence of affecting parameters such as Knudsen number, lid velocity, and velocity ratio on the flow pattern of a lid-driven cavity. Koc et al. (2021) applied event-driven molecular dynamics (EDMD) simulation to analyze the properties of mono-atomic gas flow through the porous medium in the transition regime. Molecules were considered hard sphere particles suspended in the porous medium. Based on the performed simulation, the effects of porosity, diameter of spheres, and Knudsen on mass flow rate, dynamic viscosity, tortuosity, and permeability were analyzed. Taheri et al. (2022) introduced the Symmetrized and Simplified Bernoulli Trials (SSBT) approach, which allows for greater flexibility in selecting pairs under less stringent conditions. Kalinov et al. (2022) utilized the DSMC method to simulate the kinetics of aggregation and made modifications to account for aggregation processes involving collisional fragmentation.

According to the reviewed investigations, a modified numerical approach called the MTRMC approach is proposed in this article to alleviate the CPU time of solving the Boltzmann equation. To this end, Taylor series expansion is applied to derivatives terms to obtain modified collision functions. The accuracy and computational efficiency of the MTRMC method are evaluated by considering a gas flow over a flat nano-plate as a benchmark problem. The study focuses on the following aspects of the flow:

1. Evaluating the accuracy of the MTRMC method using a test problem.
2. Comparing the required CPU times for different methods.
3. Analyzing the impact of free stream velocity on the flow pattern.

2. GOVERNING EQUATIONS

2.1 The Boltzmann Equation

The governing equation for time evolution of particles can be expressed in the form of the Boltzmann equation:

$$\frac{\partial f}{\partial t} + v.\nabla_x = \frac{1}{Kn} Q(f,f). \tag{1}$$

where $f(\boldsymbol{v},\boldsymbol{r},t)$ is the one-particle distribution function, which gives the probability density of finding a particle with velocity $\boldsymbol{v}$ at position $\boldsymbol{r}$ and time t; $Q(f,f)$ denotes the collision operator accounting for the interactions between particles. Assuming $Q(f,f) = P(f,f) - \mu f$, Eq. 1 can be rewritten as follows (Wild, 1951; Gabetta et al., 1997; Carlen et al., 2000):

$$\frac{\partial f}{\partial t} + v.\nabla_x = \frac{1}{Kn} (P(f,f) - \mu f). \tag{2}$$

The function $P(f,f)$ is a bilinear operator that exhibits symmetry and represents the interaction of molecules during collisions. The term $\mu \neq 0$ is the average collision frequency. Typically, the Boltzmann equation (2) is separated into two parts, including terms for pure convection (3) where Q is equal to zero, and the collision terms (4) where $v.\nabla_x$ is zero (Bird, 1994; Pareschi & Caflisch, 1999; Pareschi & Wennberg, 2001; Pareschi & Trazzi, 2005; Jahangiri et al., 2012). This can be mathematically expressed in the form below:

$$\frac{\partial f}{\partial t} + v.\nabla_x = 0. \tag{3}$$

$$\frac{\partial f}{\partial t} = \frac{1}{Kn} (P(f,f) - \mu f). \tag{4}$$

Equation (3) can be solved straightforwardly, which simplifies the problem to only focus on the collision part.

2.2 DSMC Method

This method involves using the Euler upwind scheme to solve equation (4) and simulate collision between particles. This scheme simplifies the problem by allowing us to focus solely on the collision step equation (4) (Pareschi & Trazzi, 2005):

$$\frac{f^{n+1}-f^{n}}{\Delta t}=\frac{\mu}{Kn}\left(\frac{P(f,f)-\mu f}{\mu}\right)-\frac{\mu}{Kn}f. \tag{5}$$

$$f^{n+1}=\left(1-\frac{\mu\Delta t}{Kn}\right)f^{n}+\frac{\mu\Delta t}{Kn}\frac{P(f,f)}{\mu}. \tag{6}$$

The DSMC method employs a probabilistic interpretation, which involves randomly sampling a particle from either f^n or $\frac{P(f,f)}{\mu}$ to obtain f^{n+1}, as given by equation (6). The former is selected with a probability of $\left(1-\frac{\mu\Delta t}{Kn}\right)$, whereas the latter is chosen with a probability of $\frac{\mu\Delta t}{Kn}$. It should be noted that the collision probability is non-negative, which requires $\frac{\mu\Delta t}{Kn}$ to be less than or equal to 1.

2.3 TRMC Method

The relaxed time τ and the transformed probability distribution function $F(v,\tau)$ is given by the following expressions, as reported in (Pareschi & Caflisch, 1999; Pareschi & Trazzi, 2005):

$$\tau=\left(1-e^{-\mu t/\mathrm{Kn}}\right). \tag{7}$$

$$F(v,\tau)=f(v,\tau)e^{-\mu t/\mathrm{Kn}}. \tag{8}$$

Accordingly, equation (4) transforms into the following expressions:

$$\frac{\partial F}{\partial \tau}=\frac{1}{\mu}P(f,f).$$

$$F(v,\tau=0)=f(v,0). \tag{9}$$

A power series solution exists for the Cauchy problem given by equation (9):

$$F(v,\tau)=\sum_{k=0}^{\infty}t^{k}f_k(v).$$

$$f(v,\tau)=e^{-\mu t/\mathrm{Kn}}\sum_{k=0}^{\infty}\left(\left(1-e^{-\mu t/\mathrm{Kn}}\right)f_k(v)\right). \tag{10}$$

By using equation (10), equation (9) can be rearranged as follows:

$$\frac{\partial F}{\partial \tau}=\sum_{k=0}^{\infty}kt^{k-1}f_k(v)=\sum_{k=0}^{\infty}(k+1)t^{k}f_{k+1}(v) \tag{11}$$

$$P(F,F)=P\left(\sum_{k=0}^{\infty}t^{k}f_k(v),\sum_{k=0}^{\infty}t^{k}f_k(v)\right)=P(f_0,f_0)+2\tau P(f_0,f_1)+\tau^{2}\left(2P(f_0,f_2)+P(f_1,f_1)\right)+\cdots \tag{12}$$

The term f_k can be calculated using a recursive algorithm by equating corresponding powers of τ:

$$f_{k+1}=\frac{1}{k+1}\sum_{h=0}^{k}\left(\frac{1}{\mu}P(f_k,f_{k-h})\right). \tag{13}$$

The TRMC approach can be derived by utilizing the Maxwellian truncation, as shown below:

$$f^{n+1}(v)=e^{-\frac{\mu\Delta t}{Kn}}\sum_{k=0}^{m}\tau^{k}f_k(v)+\left(1-e^{-\frac{\mu\Delta t}{Kn}}\right)^{m+1}M(v). \tag{14}$$

It is worth noting that the above formulations allow for the use of different weight functions. Therefore, the TRMC method in the most general form is as follows (Pareschi & Caflisch, 1999; Pareschi & Russo, 2000, 2001a, b; Pareschi & Trazzi, 2005; Trazzi et al., 2009):

$$f^{n+1}(v)=\sum_{k=0}^{m}\left(A_k f_k(v)\right)+A_{m+1}M(v). \tag{15}$$

The coefficients f_k can be determined using equation (13). In this work, the weight functions are chosen following the approach proposed by Pareschi & Russo (2000), and Pareschi & Trazzi 2005).

$$A_k=(1-\tau)\tau^{k}.$$

$$A_m=1-\sum_{k=0}^{m}A_k-A_{m+1}.$$

$$A_{m+1}=\tau^{m+2}. \tag{16}$$

This article utilizes positive weight functions are employed, which are designed to satisfy consistency, conservation, and asymptotic preservation requirements concurrently. These conditions are expressed in equations (17), (18), and (19), respectively.

$$\lim_{\tau\to 0}\frac{A_1(\tau)}{\tau}=1.$$

$$\lim_{\tau\to 0}\frac{A_k(\tau)}{\tau}=0,\ \forall k=2,\cdots,m+1. \tag{17}$$

$$\sum_{k=0}^{m+1}A_k(\tau)=1. \tag{18}$$

$$\lim_{\tau\to 1}A_k(\tau)=0,\forall k=0,\cdots,m$$

$$\lim_{\tau\to 1}A_{m+1}(\tau)=1. \tag{19}$$

It should be indicated that using lower orders of the TRMC method for large time steps may result in inaccurate results, while the higher orders of the method are computationally complex. To address this issue, the present study employs the third-order TRMC (TRMC3) method.

By setting $m=3$ in equation (15) and using the weight functions given by equation (16), the third-order TRMC scheme can be obtained.

$$f^{n+1}=(1-\tau)f_0+(\tau-\tau^{2})\frac{P(f_0,f_0)}{\mu}+(\tau^{2}-\tau^{3})\frac{P(f_0,f_1)}{\mu}+(\tau^{3}-\tau^{5})\frac{2P(f_0,f_2)+P(f_1,f_1)}{3\mu}+\tau^{5}M(v)=A_0f^{n}+A_1f_1+A_2f_2+A_3f_3+A_4M(v). \tag{20}$$

Equation (20) can be described as follows:

At the n^{th} time step, a particle can undergo one of several events according to Equation (20):

1. It may not collide with any other particle with a probability of A_0.
2. It may collide with a particle from the same population that has not undergone any collision yet, sampled from f^n, with a probability of A_1.

3. It may collide with a particle that has undergone one collision, sampled from f_1, with a probability of A_2.
4. It may undergo two collisions in the following way: first collide with another particle from the distribution f^n, followed by a subsequent collision with a particle from the distribution f_1 with a probability of $\frac{1}{3}A_3$. Alternatively, it may collide with a particle that has undergone two collisions, sampled from f_2, with a probability of $\frac{2}{3}A_3$.
5. It may be replaced by a particle sampled from a local Maxwellian distribution with a probability of A_4.

2.4 MTRMC Method

In order to modify the TRMC approach, Taylor series expansion is utilized to compute derivatives with improved accuracy.

$$\frac{\partial F}{\partial \tau} = \frac{F^{n+1}-F^n}{\Delta\tau}. \tag{21}$$

$$F^{n+1} = \sum_{k=0}^{m}(\tau+\Delta\tau)^k f_k(v). \tag{22}$$

$$\Delta\tau = \frac{\partial \tau}{\partial t}\Delta\tau = \frac{\mu\Delta t}{Kn} e^{-\frac{\mu\Delta t}{Kn}}. \tag{23}$$

The application of (21) to (23) to (9) results in derivatives represented in the following form:

$$\frac{\sum_{k=0}^{m}(\tau+\Delta\tau)^k f_k(v)-\sum_{k=0}^{m}\tau^k f_k(v)}{\Delta\tau} = \frac{1}{\mu}P(F,F). \tag{24}$$

Employing (12) to (24) gives:

$$P(F,F) = \big(P(f_0,f_0)+2\tau P(f_0,f_1)\big) + \tau^2(2P(f_0,f_2)+P(f_1,f_1)+\cdots). \tag{25}$$

The coefficients $f_k(v)$ can be determined by rearranging both sides of equation (25) so that they correspond to the same powers of the relaxation time:

$$f_1 = \frac{\Delta\tau}{(\tau+\Delta\tau)-\tau}\frac{P(f_0,f_0)}{\mu}$$

$$f_2 = \frac{2\tau\Delta\tau}{(\tau+\Delta\tau)^2-\tau^2}\frac{P(f_0,f_1)}{\mu}$$

$$f_3 = \frac{3\tau^2\Delta\tau}{(\tau+\Delta\tau)^3-\tau^3}\left(\frac{2P(f_0,f_2)+P(f_1,f_1)}{3\mu}\right)$$

$$\vdots \tag{26}$$

The MTRMC method is derived by truncating the Taylor series expansion in (10) with the coefficients f_k calculated from (26). As there are multiple choices for the weight functions, the MTRMC method can be represented in a general form.

$$f^{n+1} = \sum_{k=0}^{m} B_k f_k + B_{m+1}M(v). \tag{27}$$

Equations (6) and (27) demonstrate that the MTRMC scheme behaves similarly to the DSMC scheme in the free molecular regime where the Knudsen number is large. As the Knudsen number decreases, the collision terms become time-consuming, and the local Maxwellian distribution gradually replaces them. Additionally, as the Knudsen number becomes very small, the distribution function approaches the local Maxwellian distribution at the fluid limit.

$$\lim_{\mu\Delta t/Kn\to 0} f^{n+1} = f^n.$$

$$\lim_{\mu\Delta t/Kn\to \infty} f^{n+1} = M(v). \tag{28}$$

This study focuses on using the third order of the developed approach (hereafter called MTRMC3), which is in line with the TRMC scheme. Specifically, the MTRMC approach (27) is considered with the weight functions (16) and $m = 3$ to derive the MTRMC3 scheme, which is expressed as follows:

$$f^{n+1} = (1-\tau+\varepsilon)f^n + (\tau-\tau^2)\frac{P(f_0,f_0)}{\mu} + (\tau^2-\tau^3)\left(\frac{2\tau}{2\tau+\Delta\tau}\right)\frac{P(f_0,f_1)}{\mu} + (\tau^3 - \tau^5)\left(\frac{3\tau^2}{3\tau^2+3\tau\Delta\tau+\Delta\tau^2}\right)\frac{2P(f_0,f_2)+P(f_1,f_1)}{3\mu} + \tau^5 M(v)$$
$$= B_0 f^n + B_1 f_1 + B_2 f_2 + B_3 f_3 + B_4 M. \tag{29}$$

where $\varepsilon = (\tau - B_1 - B_2 - B_3 - B_4) > 0$. The MTRMC method has a key advantage over the DSMC method as it can accept larger time steps. This is because the DSMC method has a time step limit of $\mu\Delta t/Kn \leq 1$, which is not present in the MTRMC method due to the use of relaxed time and transformed probability distribution functions. Additionally, the MTRMC method has modified collision functions resulting in smaller number of collisions between molecules compared to the TRMC method. As a result, the MTRMC method has lower computational expense than the TRMC method. The flowchart of the MTRMC3 approach is shown in Fig. 1.

3. THE GEOMETRY AND CALCULATION CONDITION

The present study aims to examine the computational efficiency and precision of the MTRMC scheme in contrast to the TRMC and DSMC schemes. Specifically, the study focuses on the flow of Argon over a flat nano-plate. The objective is to evaluate the performance of MTRMC and compare it with the other two schemes in terms of accuracy and computational costs.

Figure 2 illustrates the geometry and the applied boundary conditions. It should be indicated that all boundaries except for the plate surface are assumed to be free streams. The plate surface is modeled as a diffuse reflector (Jahangiri et al., 2012; Amiri-Jaghargh et al., 2013; Darbandi & Roohi, 2013; Watvisave et al., 2015), except for the specular reflector, which is located at the initial 10% of the nano-plate's length. The inclusion of a specular boundary upstream of the leading edge results in a more realistic inlet velocity distribution (Bird, 1994; Darbandi & Schneider, 1997; Darbandi & Vakilipour, 2009; Vakilipour & Darbandi, 2009; Darbandi & Roohi, 2013;Watvisave et al., 2015). The length L and height h of the model are specified as $100\,nm$ and $60\,nm$,

respectively. The cells are uniform horizontally, but geometrically progress vertically.

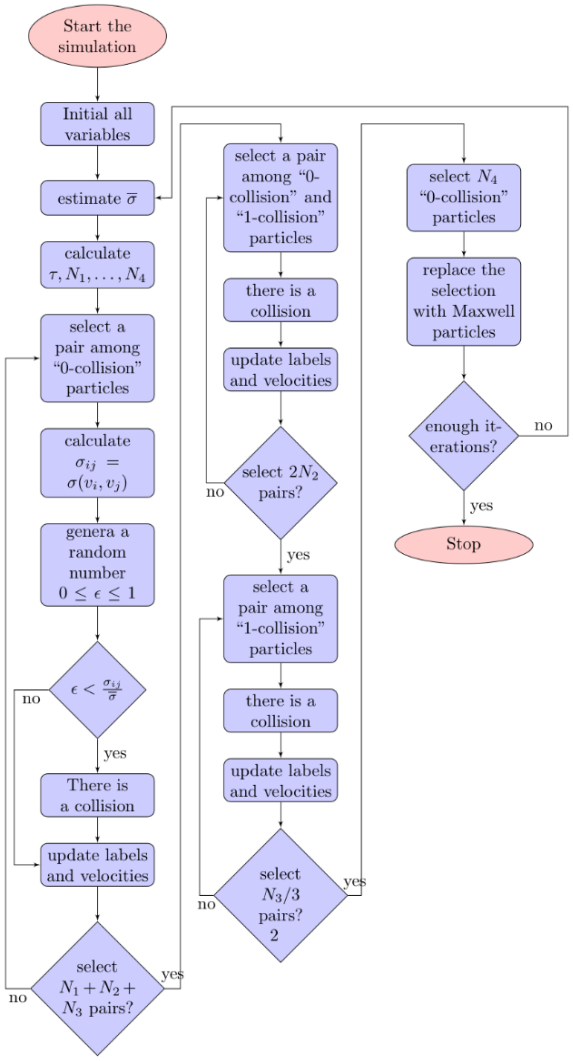

Fig. 1 Flowchart of the MTRMC3 approach

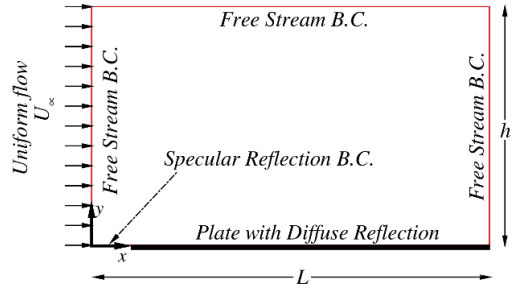

Fig. 2 Geometry and boundary conditions of flat nano-plate

The free stream is composed of mono-atomic Argon that flows along the x-axis at a temperature of $300K$. The surface temperature is set at $500K$. In this study, three free stream velocities ($14m/s$ for case I, $141m/s$ for case II, and $1412m/s$ for case III) are considered in simulations. These velocities are chosen to analyze the behavior of the nano-plate under flows ranging from low subsonic to supersonic velocities. The Knudsen number, inlet pressure, and number density of the free stream flow are specified as 0.00129, $41.4\,MPa$, and $10^{28}mol/m^3$, respectively. The Knudsen number is an indicator reflecting the rarefaction degree of the flow. The inter-molecular collisions are simulated using the variable hard sphere (VHS) model. During the simulations, viscosity index, and the molecular diameter and mass are set to 0.81, $4.17 \times 10^{-17}m$, and $66.3 \times 10^{-27}kg$, respectively (Bird, 1994).

In the DSMC scheme, the time step is calculated based on the constraint $\mu\Delta t/Kn \le 0$ (see equation (6)), while this parameter in the TRMC and MTRMC schemes is set as a fraction of the free flow time step, $C\Delta t$, in which $C \le 1$. For the current study, the value of C is selected as 0.41, 0.35, and 0.18 for cases I to III, respectively.

3.1 Grid Independence Analysis

To obtain accurate results, finer cells are required, but at the cost of higher computational CPU time. Therefore, a grid independence analysis is conducted using different grid resolutions: 300×60, 300×180, 300×360, 300×540, 300×720 cells. The cells are refined in the vertical direction, as the variation of flow properties in the longitudinal direction is small (LeBeau et al., 2003; Shen et al., 2003; Darbandi & Roohi, 2013).

This research investigates the variations of velocity, pressure, and temperature distributions across a nano-plate using different grid resolutions. The findings suggest that compared to temperature and velocity distributions, pressure distributions are less affected by cell size. The outcomes also indicate that slip velocity and temperature distributions remain unaffected with grid resolutions finer than 300×540. Nonetheless, to ensure grid resolution independence, the study employs a grid resolution of 300×720. To ensure accuracy, a minimum of 20 particles per cell is used, resulting in 4,400,000 particles being considered. The results suggest that the chosen grid resolution and particle number are appropriate for accurate analysis. Figure 3 provides visual representation of the comparison of pressure, velocity, and temperature distributions over the nano-plate for different grid resolutions.

4. COMPARATIVE ANALYSIS OF RESULTS OBTAINED FROM DIFFERENT SIMULATION SCHEMES FOR NANO-PLATE FLOW

This section presents the findings of the MTRMC scheme and compares them with those obtained from the DSMC, TRMC, and hybrid DSMC-NS schemes. The results are presented at $x/L = 0.2$ and 0.8 normal to the nano-plate in addition to those over the nano-plate to examine the problem more accurately. The aim of this comparison is to validate the MTRMC scheme and to gain more insight into the problem.

In Fig. 4, a comparison is presented between the temperature distributions obtained by using the MTRMC scheme and the DSMC and TRMC schemes for case I with a free stream velocity of $U_\infty = 14m/s$. The results show that there is a good agreement between the temperature distributions obtained from different schemes.

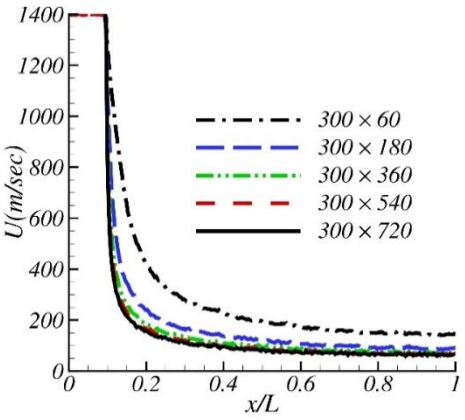

(a) Slip velocity on the plate surface

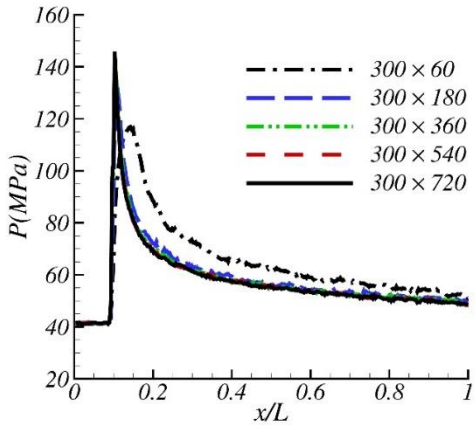

(b) Pressure curves on the plate surface

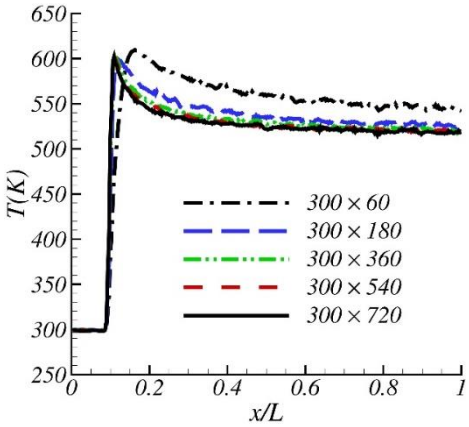

(c) Temperature curves on the plate surface

Fig. 3 Grid independency tests

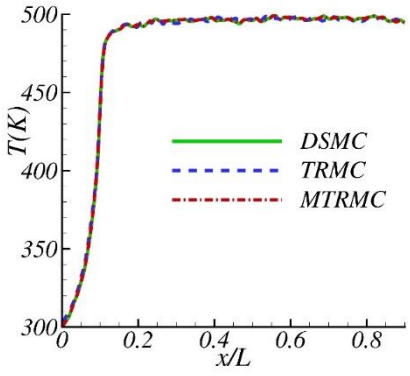

(a) Distribution of temperature across the plate surface

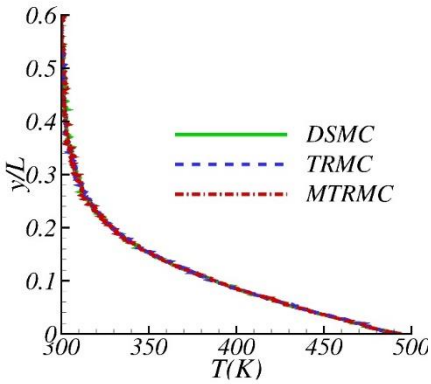

(b) Temperature distributions at $x/L = 0.2$

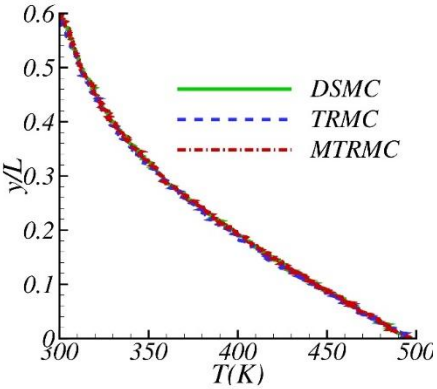

(c) Temperature distribution at $x/L = 0.8$

Fig. 4 Comparison of the results obtained from different schemes when $U_\infty = 14\,m/s$

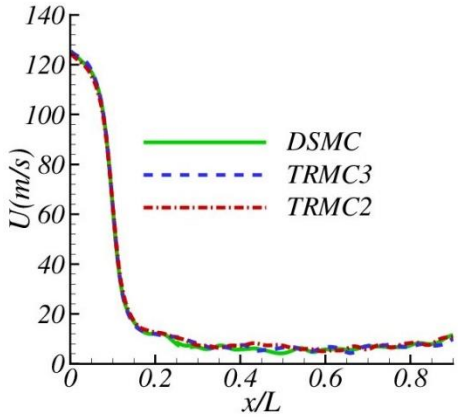

(a) Velocity distributions

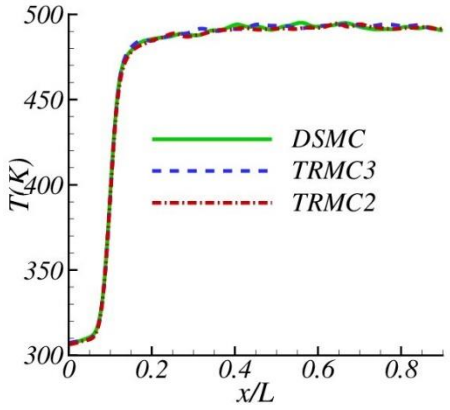

(b) Temperature profiles

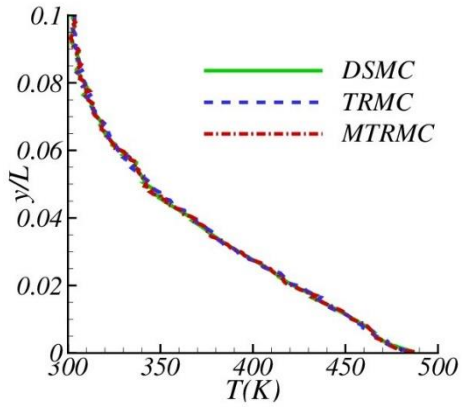

(c) Temperature distributions at $x/L = 0.2$

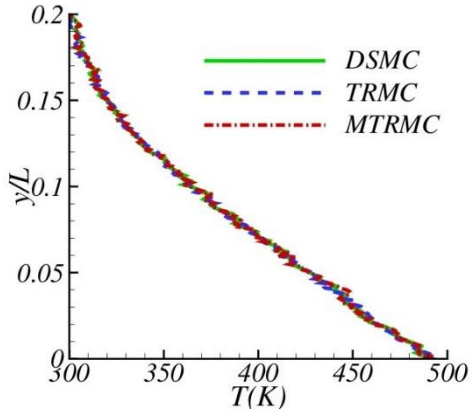

(d) Temperature distributions at $x/L = 0.8$

Fig. 5 Temperature and velocity distributions when $U_\infty = 141\, m/s$

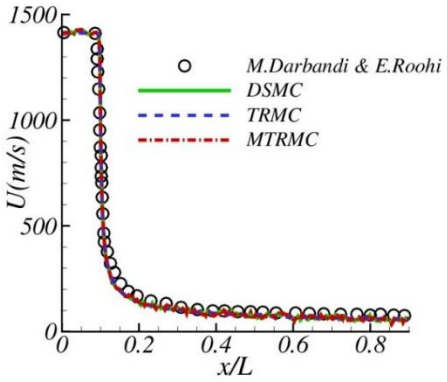

(a) Velocity distributions

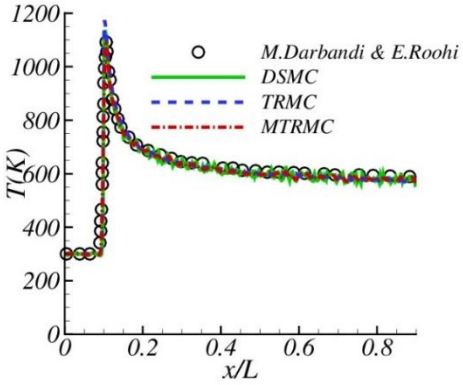

(b) Temperature distributions

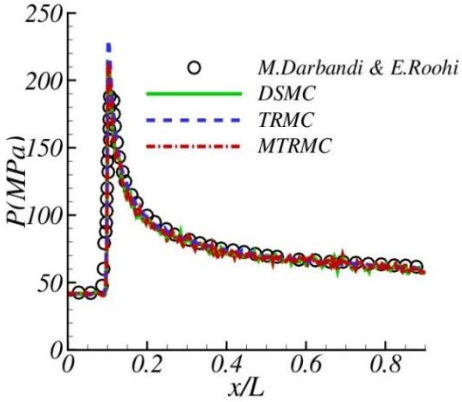

(c) Pressure distributions

Fig. 6 Comparison of the results obtained from different techniques for a scenario with a free stream velocity of $U_\infty = 1412\, m/s$

Figure 5 displays the temperature distributions perpendicular along the x-axis over the plate and along the y-axis at $x/L = 0.2$ and 0.8, and $U_\infty = 14 m/s$. A comparison between the MTRMC scheme and the conventional DSMC and TRMC schemes indicates a significant level of resemblance.

Figures 6 and 7 demonstrate a comparison between the outcomes of various approaches for a scenario with a free stream velocity of $U_\infty = 1412\, m/s$. Besides, the pressure, temperature, and velocity distributions are studied at different longitudinal distances to examine the problem more accurately. The results reveal a remarkable similarity between the results obtained from the MTRMC, DSMC, TRMC, and hybrid DSMC-NS techniques.

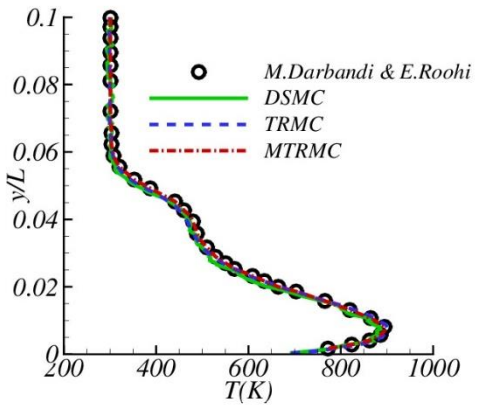

(a) Temperature distributions at $x/L = 0.2$

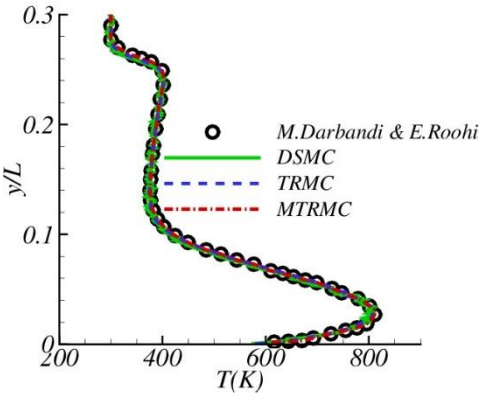

(b) Temperature distributions at $x/L = 0.8$

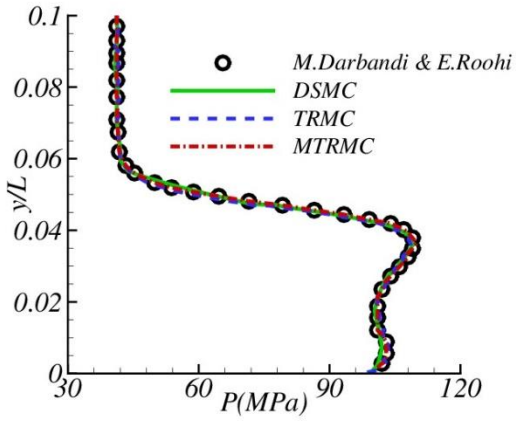

(c) Pressure distributions at $x/L = 0.2$

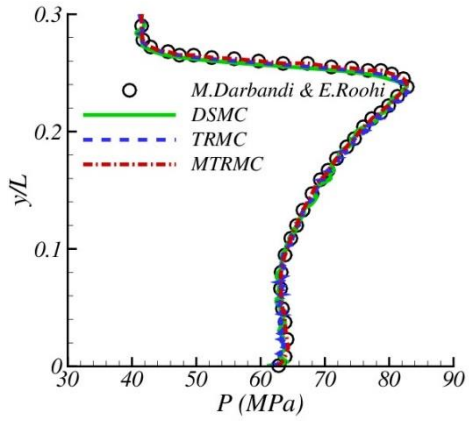

(d) Pressure distributions at $x/L = 0.8$

Fig. 7 Comparison of the results at different locations (x/L = 0.2 and 0.8) obtained from different schemes for the scenario with $U_\infty = 1412\ m/s$

Based on Fig. 6, it can be inferred that the slip velocity at the front edge of the nano-plate is comparable to the velocity of the free stream. The slip velocity gradually decreases along the length of the nano-plate, but it does not completely vanish. Moreover, the temperature and pressure distributions exhibit a significant jump at the leading edge of the nano-plate; however, such jumps decrease along the length of the nano-plate. It is notable that the jump in the pressure distributions diminishes almost entirely along the length of the nano-plate, whereas the temperature asymptotically remains considerably higher than both the wall and free stream temperatures. This phenomenon may originate from the creation of an oblique shock wave over the nano-plate in this case study with $U_\infty = 1412\ m/s$.

In Fig. 7, the pressure and temperature along the y-axis at different locations are investigated. The results indicate that the maximum temperature for each temperature distribution exceeds the temperature of the surface of the nano-plate or the free stream flow, and it is located in close proximity to the surface of the nano-plate. This observation may suggest that the oblique shock wave discussed earlier is formed near the surface of the nano-plate. Comparing the obtained results with those reported by Darbandi and Roohi (Darbandi & Roohi, 2013) reveals that the MTRMC approach is capable of accurately simulating the shock wave.

Figures 4 through 7 clearly show that the MTRMC approach produces results that are consistent with the TRMC and DSMC methods when simulating the flow of Argon over a nano-plate at various free stream velocities, ranging from low (i.e. $U_\infty = 14\,m/s$) to supersonic (i.e. $U_\infty = 1412\,m/s$).

In Fig. 8, the consumed computational CPU time is plotted against the physical time at various free stream velocities for various approaches. The comparisons reveal that, for the same physical time, the MTRMC approach requires significantly less computational CPU time than the DSMC and TRMC approaches. The significant difference in computational expenses between the MTRMC and the DSMC schemes is due to the replacement of intermolecular collisions with the local Maxwellian distribution, as well as the use of the relaxed time (τ) which allows for the utilization of higher time steps (as seen in (6) and (29)). Furthermore, the improved computational efficiency of the MTRMC scheme, as compared to the TRMC approach, originate from modified collision functions that involve a smaller number of collisions between molecules (as shown in (20) and (29)).

Table 1 shows the normalized computational CPU times for various approaches at different free stream velocities. The normalization process is conducted utilizing data of the DSMC approach. The table reveals that the computational CPU time required by the MTRMC scheme to simulate a plate subjected to a free stream is significantly less than that required by the DSMC and TRMC approaches. This difference is more prominent when the comparison is made with the computational CPU time of the DSMC method.

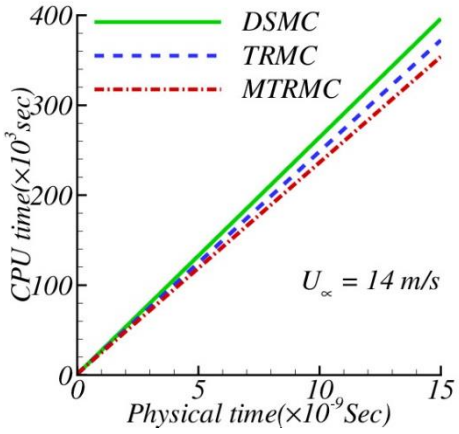

(a) Case I ($U_\infty = 14\,m/s$)

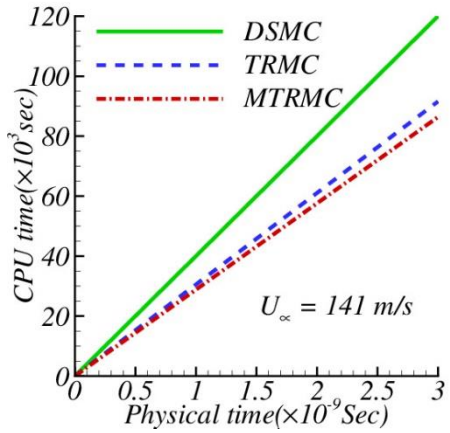

(b) Case II ($U_\infty = 141\,m/s$)

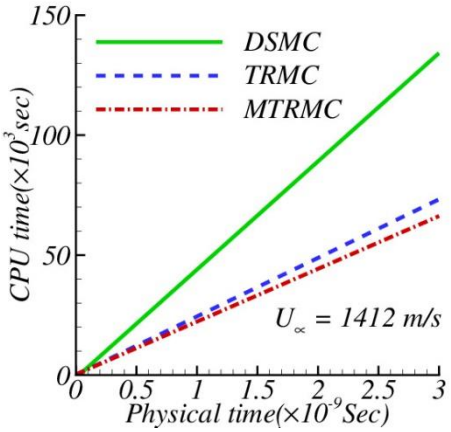

(c) Case III ($U_\infty = 1412\,m/s$)

Fig. 8 Computational expenses of different schemes under various free stream velocities

Table 1 Normalized computational CPU times for different schemes under different free stream velocities

U_∞	Normalized CPU time				
	$14\,m/s$	$141\,m/s$	$500\,m/s$	$800\,m/s$	$1000\,m/s$
DSMC	1.000	1.000	1.000	1.000	1.000
TRMC	0.940	0.774	0.595	0.572	0.547
MTRMC	0.894	0.730	0.561	0.533	0.498

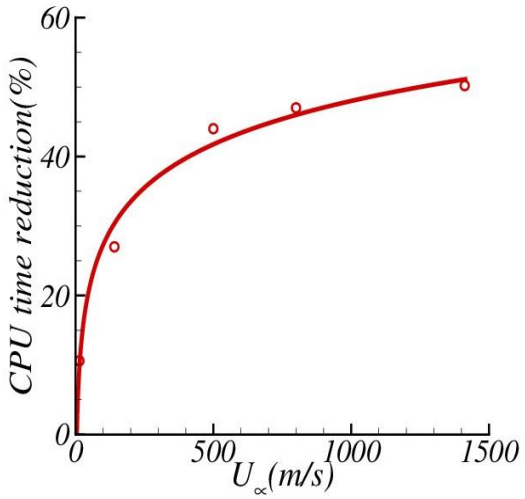

Fig. 9 Comparison of CPU time in MTRMC and DSMC techniques

Figure 9 shows the percentage alleviation in the required computational CPU time for the MTRMC scheme compared to the DSMC scheme. The results indicate that the reduction in CPU time increases significantly with increasing free stream velocity. For free stream velocities above $1000\,m/s$, the alleviation in CPU time reaches an asymptotic value of approximately 53%.

5. COMPARISON OF THE RESULTS FOR VARIOUS CASES

The MTRMC scheme produced streamlines overlaid on temperature contours for various stream velocities in Fig. 10. The findings suggest that the peak temperature significantly increases with increasing free stream velocity, with the exception of case I where the temperature increase is minimal. For case III, a hot spot emerges near the nano-plate's leading edge, possibly due to presence of a shock wave. The downstream streamlines are more impacted by the nano-plate at lower free stream velocities, potentially due to the larger velocity boundary layer. Overall, the results from the MTRMC scheme offer valuable insights into the behavior of the nano-plate exposed to the free Argon flow under diverse flow conditions.

Distributions of shear stress, velocity, and temperature over the nano-plate under various free stream velocities are presented in Fig. 11.

The slip velocity is defined as the difference between the velocity of the fluid in the vicinity of the surface of the nano-plate and the velocity of the surface of the nano-plate. The slip velocity distributions over the nano-plate obtained from the MTRMC scheme for various free stream velocities are presented in Fig. 11. The slip velocity distributions show that the maximum slip velocity over the surface of the nano-plate increases as the free stream velocity increases. This indicates that the effect of the slip velocity becomes more significant for higher free stream velocities.

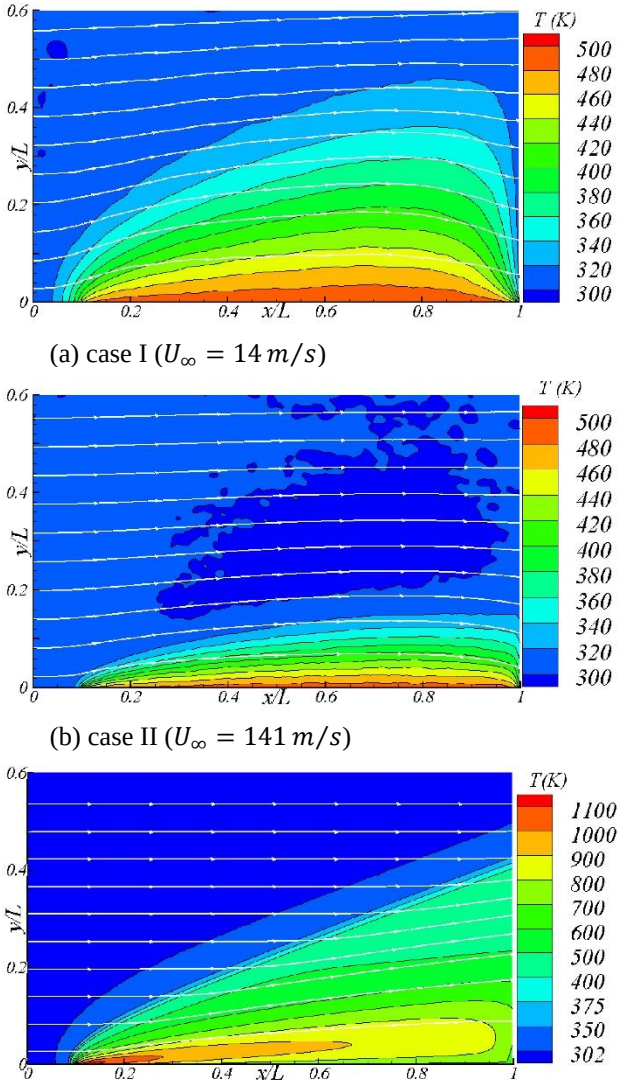

(a) case I ($U_\infty = 14\,m/s$)

(b) case II ($U_\infty = 141\,m/s$)

(c) case III ($U_\infty = 1412\,m/s$)

Fig. 10 Velocity streamlines and temperature contours in different scenarios

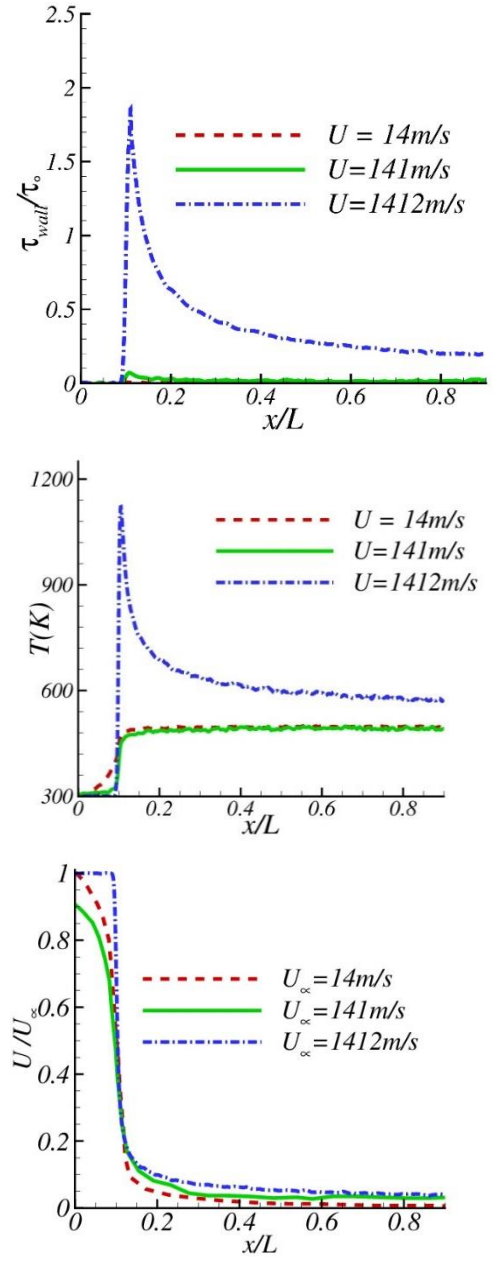

Fig. 11 Temperature contours and streamlines in the studied cases

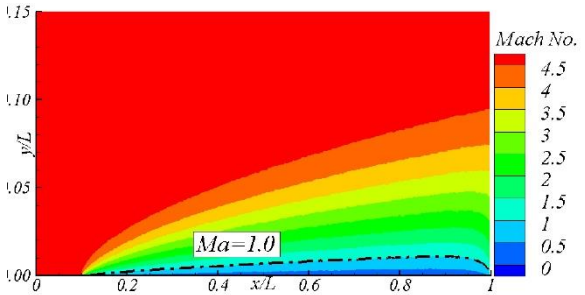

Fig. 12 Contour of local Mach number in case III

The rapid increase in temperature and pressure distributions and the resulting hot spot in case III can be explained by the formation of an oblique shock wave due to the supersonic free stream velocity ($U_\infty = 1412\,m/s$). Figure 12 shows the contours of the local Mach number for case III with the $Ma = 1$ isoline highlighted, revealing that the shock wave is formed very near the plate surface.

6. CONCLUSION

This article focuses on the development of the MTRMC scheme. To this end, Taylor series expansion was applied to the Wild function to modify collision terms and achieve accurate results with a smaller number of collisions between molecules. The MTRMC scheme was applied to accurately simulate the flow of free stream Argon over a nano-plate, covering a range of free stream velocities from low subsonic to supersonic. The results showed that the MTRMC scheme was capable of accurately simulating the flow at all velocities tested.

Additionally, it was found that the CPU time of the MTRMC scheme was significantly lower than that of the DSMC and TRMC schemes for the same physical time. The reduction in CPU time was more pronounced at higher free stream velocities, and the MTRMC scheme showed up to a 51% reduction in CPU time compared to the DSMC scheme. Overall, the results demonstrated that the MTRMC scheme could be a more efficient and

accurate method for simulating rarefied gas flows over surfaces at a range of free stream velocities.

CONFLICT OF INTEREST

The authors of this article declare that they have no conflicts of interest to disclose.

AUTHORS CONTRIBUTION

M. Eskandari: Conceptualization; Code developing; Writing the original draft. **S. S. Nourazar**: Conceptualization; Supervision writing; Review and editing.

REFERENCES

Amiri-Jaghargh, A., Roohi, E., Niazmand, H., & Stefanov, S. (2013). DSMC simulation of low knudsen micro/nanoflows using small number of particles per cells. *Journal of Heat Transfer*, *135*(10). https://doi.org/10.1115/1.4024505

Baliti, J., Hssikou, M., & Alaoui, M. (2019). Gas flow and heat transfer in an enclosure induced by a sinusoidal temperature. *Journal of Applied Fluid Mechanics*, *12*(6), 1757-1767. https://doi.org/10.29252/jafm.12.06.29304

Bird, G. A. (1994). Molecular gas dynamics and the direct simulation of gas flows. *Molecular Gas Dynamics and the Direct Simulation of Gas Flows*.

Carlen, E., Carvalho, M., & Gabetta, E. (2000). Central limit theorem for Maxwellian molecules and truncation of the Wild expansion. *Communications on Pure and Applied Mathematics: A Journal Issued by the Courant Institute of Mathematical Sciences*, *53*(3), 370-397. https://doi.org/10.1002/(SICI)1097-0312(200003)53:3%3C370::AID-CPA4%3E3.0.CO;2-0

Cercignani, C., & Cercignani, C. (1988). *The boltzmann equation*. Springer. https://doi.org/10.1007/978-1-4612-1039-9_2

Darbandi, M., & Roohi, E. (2013). A hybrid DSMC/Navier–Stokes frame to solve mixed rarefied/nonrarefied hypersonic flows over nano-plate and micro-cylinder. *International Journal for Numerical Methods in Fluids*, *72*(9), 937-966. https://doi.org/10.1002/fld.3769

Darbandi, M., & Schneider, G. (1997). Momentum variable procedure for solving compressible and incompressible flows. *AIAA Journal*, *35*(12), 1801-1805. https://doi.org/10.2514/2.45

Darbandi, M., & Vakilipour, S. (2009). Solution of thermally developing zone in short micro-/nanoscale channels. *Journal of heat Transfer*, *131*(4). https://doi.org/10.1115/1.3072908

Dimarco, G., & Pareschi, L. (2011). Exponential runge–kutta methods for stiff kinetic equations. *SIAM Journal on Numerical Analysis*, *49*(5), 2057-2077. https://doi.org/10.1137/100811052

Eskandari, M., & Nourazar, S. (2017). On the time relaxed Monte Carlo computations for the lid-driven micro cavity flow. *Journal of Computational Physics*, *343*, 355-367. https://doi.org/10.1016/j.jcp.2017.03.017

Eskandari, M., & Nourazar, S. (2018a). On the Expedient solution of the boltzmann equation by modified time relaxed monte carlo (MTRMC) method. *Journal of Applied Fluid Mechanics*, *11*(3), 655-666. https://doi.org/10.29252/jafm.11.03.28007

Eskandari, M., & Nourazar, S. (2018b). On the time relaxed Monte Carlo computations for the flow over a flat nano-plate. *Computers & Fluids*, *160*, 219-229. https://doi.org/10.1016/j.compfluid.2017.10.021

Filbet, F., & Russo, G. (2003). High order numerical methods for the space non-homogeneous Boltzmann equation. *Journal of Computational Physics*, *186*(2), 457-480. https://doi.org/10.1016/S0021-9991(03)00065-2

Gabetta, E., Pareschi, L., & Toscani, G. (1997). Relaxation schemes for nonlinear kinetic equations. *SIAM Journal on Numerical Analysis*, *34*(6), 2168-2194. https://doi.org/10.1137/S0036142995287768

Ganjaei, A., & Nourazar, S. (2009). Numerical simulation of a binary gas flow inside a rotating cylinder. *Journal of mechanical Science and Technology*, *23*, 2848-2860. https://doi.org/10.1007/s12206-008-1210-2

Jahangiri, P., Nejat, A., Samadi, J., & Aboutalebi, A. (2012). A high-order Monte Carlo algorithm for the direct simulation of Boltzmann equation. *Journal of Computational Physics*, *231*(14), 4578-4596. https://doi.org/10.1016/j.jcp.2012.02.029

Kalinov, A., Osinsky, A., Matveev, S. A., Otieno, W., & Brilliantov, N. V. (2022). Direct simulation Monte Carlo for new regimes in aggregation-fragmentation kinetics. *Journal of Computational Physics*, *467*, 111439. https://doi.org/10.1016/j.jcp.2022.111439

Koç, M., Kandemir, İ., & Akkaya, V. R. (2021). An investigation of transition flow in porous media by event driven molecular dynamics simulation. *Journal of Applied Fluid Mechanics*. https://doi.org/10.47176/jafm.14.01.31475

LeBeau, G., Jacikas, K., & Lumpkin, F. (2003). *Virtual sub-cells for the direct simulation Monte Carlo method*. 41st Aerospace Sciences Meeting and Exhibit, https://doi.org/10.2514/6.2003-1031

Mukherjee, S., Shahabi, V., Gowtham, R., Rajan, K., & Velamati, R. (2019). Effect of knudsen number, lid velocity and velocity ratio on flow features of single and double lid driven cavities. *Journal of Applied Fluid Mechanics*, *12*(5), 1575-1583. https://doi.org/10.29252/jafm.12.05.29335

Oran, E. S., Oh, C., & Cybyk, B. (1998). Direct simulation Monte Carlo: recent advances and applications. *Annual Review of Fluid Mechanics*, *30*(1), 403-441. https://doi.org/10.1146/annurev.fluid.30.1.403

Pan, L., Liu, G., Khoo, B., & Song, B. (2000). A modified direct simulation Monte Carlo method for low-speed microflows. *Journal of Micromechanics and Microengineering*, *10*(1), 21. https://doi.org/10.1088/0960-1317/10/1/304

Pareschi, L., & Caflisch, R. E. (1999). An implicit Monte Carlo method for rarefied gas dynamics: I. The space homogeneous case. *Journal of Computational Physics*, *154*(1), 90-116. https://doi.org/10.1006/jcph.1999.6301

Pareschi, L., & Russo, G. (2000). Asymptotic preserving Monte Carlo methods for the Boltzmann equation. *Transport Theory and Statistical Physics*, *29*(3-5), 415-430. https://doi.org/10.1080/00411450008205882

Pareschi, L., & Russo, G. (2001a). *An introduction to Monte Carlo method for the Boltzmann equation*. ESAIM: Proceedings.

Pareschi, L., & Russo, G. (2001b). Time relaxed Monte Carlo methods for the Boltzmann equation. *SIAM Journal on Scientific Computing*, *23*(4), 1253-1273. https://doi.org/10.1137/S1064827500375916

Pareschi, L., & Trazzi, S. (2005). Numerical solution of the Boltzmann equation by time relaxed Monte Carlo (TRMC) methods. *International Journal for Numerical Methods in Fluids*, *48*(9), 947-983. https://doi.org/10.1002/fld.969

Pareschi, L., & Wennberg, B. (2001). A recursive Monte Carlo method for the Boltzmann equation in the Maxwellian case. https://doi.org/10.1515/mcma.2001.7.3-4.349

Plimpton, S., Moore, S., Borner, A., Stagg, A., Koehler, T., Torczynski, J., & Gallis, M. (2019). Direct simulation Monte Carlo on petaflop supercomputers and beyond. *Physics of Fluids*, *31*(8), 086101. https://doi.org/10.1063/1.5108534

Russo, G., Pareschi, L., Trazzi, S., Shevyrin, A., Bondar, Y. A., & Ivanov, M. (2005). *Plane Couette flow computations by TRMC and MFS methods*. AIP Conference Proceedings, https://doi.org/10.1063/1.1941598

Shen, C., Fan, J., & Xie, C. (2003). Statistical simulation of rarefied gas flows in micro-channels. *Journal of Computational Physics*, *189*(2), 512-526. https://doi.org/10.1016/S0021-9991(03)00231-6

Taheri, E., Roohi, E., & Stefanov, S. (2022). A symmetrized and simplified Bernoulli trial collision scheme in direct simulation Monte Carlo. *Physics of Fluids*, *34*(1), 012010. https://doi.org/10.1063/5.0076025

Trazzi, S., Pareschi, L., & Wennberg, B. (2009). Adaptive and recursive time relaxed monte carlo methods for rarefied gas dynamics. *SIAM Journal on Scientific Computing*, *31*(2), 1379-1398. https://doi.org/10.1137/07069119X

Vakilipour, S., & Darbandi, M. (2009). Advancement in numerical study of gas flow and heat transfer in a microscale. *Journal of Thermophysics and Heat Transfer*, *23*(1), 205-208. https://doi.org/10.2514/1.37037

Watvisave, D. S., Puranik, B. P., & Bhandarkar, U. V. (2015). A hybrid MD-DSMC coupling method to investigate flow characteristics of micro-devices. *Journal of Computational Physics*, *302*, 603-617. https://doi.org/10.1016/j.jcp.2015.09.012

Wild, E. (1951). *On Boltzmann's equation in the kinetic theory of gases.* Mathematical Proceedings of the cambridge Philosophical society. https://doi.org/10.1017/S0305004100026992